Clean Technologies and Recycling

Clean Technologies and Recycling, 3(4): 267–282.
DOI: 10.3934/ctr.2023017
Received: 01 November 2023
Revised: 05 December 2023
Accepted: 11 December 2023
Published: 27 December 2023

http://www.aimspress.com/journal/ctr

Research article

Performance evaluation of oscillatory baffle Bunsen reactor in iodine sulfur thermochemical process for hydrogen production

V Nafees Ahmed* and A Shriniwas Rao

BARC, Mumbai, India

*** Correspondence:** Email: nafeesva@barc.gov.in.

Abstract: Hydrogen is an environmentally attractive transportation fuel that can replace fossil fuels. The iodine-sulfur (I-S) thermo-chemical process involves three reaction steps. The Bunsen reaction is one of the main reaction steps of I-S process and plays an important role in defining overall process efficiency. Different types of reactors are being studied, including the oscillatory baffle Bunsen reactor. The reactor selection is based on process intensification and process integration, i.e., reaction and separation in the single equipment. Simulations are performed for two-dimensional cases by solving incompressible Navier-Stokes equations along with continuity equation, the geometry chosen is of single section in the column and diameter of 50 mm and baffle spacing of 50, 75, 100 mm i.e. 1, 1.5 and 2 times the diameter of column and baffle free area 22%. The residence time distribution experiments are carried out in a metallic reactor with NaCl as a tracer operated at different frequencies, amplitudes and flow rates. D/uL is evaluated from experimental curves. The power per unit mass is compared for oscillatory baffled column and stirred tank for a semi-batch process. From the numerical simulations, good eddy interactions are present at higher frequencies and amplitudes and at a baffle spacing of 1.5 times the diameter of the column. Residence time distribution analysis gives a lower dispersion number at medium frequencies and higher amplitudes with constant flow rate. If the flow rates are high, then it is better to operate at higher frequencies and amplitudes to achieve plug flow behavior. Power per unit mass is less for oscillatory baffle column compared to the stirred tank of given configuration. With better mixing performance and less power per unit volume, the oscillatory baffle column is a good alternative to other columns.

Keywords: hydrogen energy; iodine-sulfur process; hydrogen; oscillatory flow

Nomenclature: C: concentration; d: pipe diameter; d_o: Baffle opening diameter; D: axial dispersion coefficient; L: length of column; N: baffle spacing; p: pressure; Re_p: pulsating Reynolds number; Re_o: oscillatory Reynolds number; *St*: Strouhal number; *t*: time; $\bar{t}$: mean time of passage; u: superficial flow velocity; u_p: pulsating velocity; u_{peak}: peak velocity at the maximum channel width; Vr: fluid velocities at r coordinate; V_θ: fluid velocities at θ coordinate; Vz: fluid velocities at z coordinate; x_o: amplitude; D/uL: vessel dispersion number; σ^2: variance, or a measure of the spread of the curve; μ: dynamic viscosity of fluid; ρ: density of the fluid; ω: angular frequency of oscillation; Co: inlet concentration of solute; S: baffle free area; n: impeller rotation speed; d_a: impeller diameter; K_T: power number; V: volume of fluid in the tank; P/M: power per unit mass

1. Introduction

Hydrogen is considered a clean transportation fuel that has the potential to dislodge fossil fuels [1]. Presently, hydrogen production is primarily based on fossil fuels. Hydrogen is generated by various means including thermochemical method by splitting water.

Iodine-sulfur (I-S) process is one of the thermochemical processes being studied world over [2]. Bunsen reaction is one of the three main reaction steps of I-S process and can be considered as the critical step in terms of overall process feasibility and stability [3]. In this step, water is reacted with iodine (I_2) and sulfur dioxide (SO_2) to obtain hydriodic acid and sulfuric acid. Excess water and iodine are used to make the reaction and product phase separation feasible [4]. The two products of the Bunsen reaction form two immiscible phases [5]. The Bunsen reaction is multiphase, reversible and exothermic in nature [6]. Therefore, efficient mixing is required to maintain the desired temperature of the reactor and to enhance the transfer coefficients [7]. For that purpose, different types of reactors are being studied, including the oscillatory baffle Bunsen reactor. The reactor selection is based on process intensification and process integration, i.e., reaction and separation in the single equipment [8]. Process intensification is a method which results in compact, safe and energy efficient know-how without affecting the performance [9]. Effective transportation of mass and energy and good fluid mixing are necessary in many process tasks. These conditions are regularly achieved by incorporating turbulence, and these can be attained by high flow rates or installing baffles, constrictions, etc. In a batch process, mixing is provided to enhance heat or mass transfer or to achieve uniform conditions for a reaction. This is generally obtained using an agitator. An oscillatory flow gives an effective, different means of agitation and provides a range of specific process improvements that intensify the process [10]. Initially, oscillatory flows or pulsating flows were utilized in the mid-20th century in the nuclear industry for solvent extraction [10].

The basic phenomenon for mixing augmentation is the formation and dissipation of cyclic distinct vortices in the bulk fluid. This can be applied in single and multiphase systems provided the fluid is the principal phase. The periodical reversing fluid motion interacts with the baffles, forming vortices. Particularly, the resultant radial and axial velocities are of the same magnitude, providing effective and unvarying mixing in the zones between consecutive baffles [11]. Figure 1 shows the basic configuration of an oscillatory baffle Bunsen reactor (OBBR) with two types of oscillation mechanisms (Figure 1) and the typical flow patterns captured in a tube where the fluid is subjected to an enforced oscillatory motion. It is clear from Figure 2a that no benefit is obtained by imposing oscillations when a smooth tube is used. Figure 2b shows the flow patterns in a baffled tube subject

to moderate oscillatory conditions. The vortices can be clearly seen. In Figure 2c, the effect of high oscillation can be seen, the flow is now turbulent. The important aspect of oscillating baffled flow is that mixing can be tuned to a high degree of precision, giving a varying range of mixing conditions, from 'soft' mixing (Figure 2b), exhibiting plug flow characteristics, to the most intense (Figure 2c), approaching mixed flow conditions [11]. A device which employs this mixing is usually called a pulsed flow reactor (PFR), an oscillatory flow reactor (OFR) or an oscillatory baffled column (OBC) [12]. Therefore, the reactor for the present application is named the oscillatory baffle Bunsen reactor (OBBR).

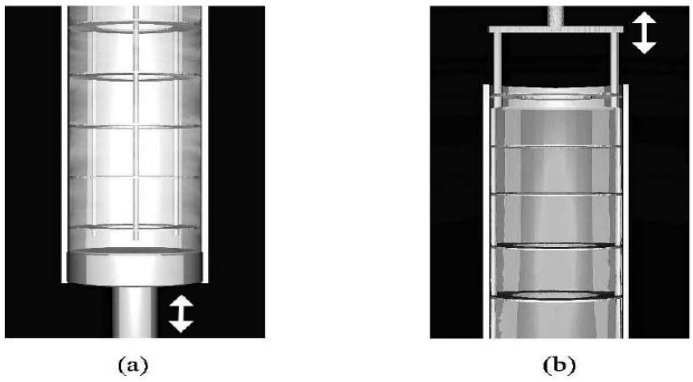

Figure 1. Oscillatory baffle column/reactor with two different mechanisms for generation of oscillations.

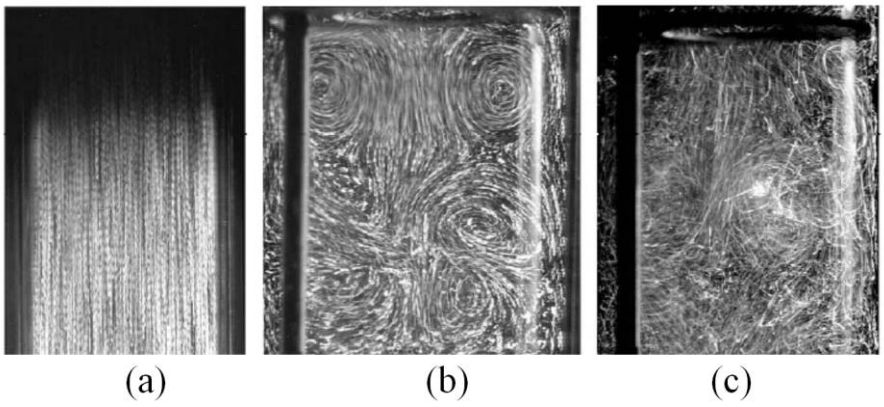

Figure 2. (a) Flow in the smooth tube with oscillations and without baffles; (b) Flow in tube with baffles and oscillations; (c) Flow in tube with baffles and oscillations at high frequency and amplitude.

2. Materials and methods

2.1. Operating parameters

The classical dimensionless group for pipe flows is the well-known Reynolds number and is defined as the ratio of inertial force to viscous force in the flow,

$$Re = \frac{\rho u d}{\mu} \quad (1)$$

where *D* is the pipe diameter, μ the dynamic viscosity of fluid, ρ is the density of the fluid and *u* the mean superficial flow velocity.

The fluid mechanics of OBBR are described by two dimensionless groups, which were reported by [13,14], referring the first group as the oscillatory Reynolds number, Re_o,

$$Re_o = \frac{\omega x_o \rho d}{\mu} \quad (2)$$

and the second group as the Strouhal number

$$St = \frac{d}{4\pi x_o} \quad (3)$$

The oscillatory Reynolds number describes the intensity of mixing applied to the column. The Strouhal number is initiated in studies of vortex shedding for flow around objects and through orifices or similar restrictions. Here, the Strouhal number describes the effective eddy propagation.

2.2. Geometrical parameters

2.2.1. Baffle spacing

Baffle spacing is also an important parameter in oscillatory flows. It is defined in terms of the diameter of the column, dictates the number of vortex formation in the reactor/column and is the ratio of spacing between the baffles to column diameter.

$$\text{Baffle spacing, } N = L/d \quad (4)$$

2.2.2. Baffle free area

Baffle free area is also another important geometrical parameter in oscillatory flow. It is defined as the ratio of the square of the diameter of the baffle opening to square of column diameter. It dictates the depth of vortex generation in the inter baffle regions.

$$\text{Baffle free area} = d_o^2/d^2 \quad (5)$$

2.3. Numerical simulation set-up and procedure

2.3.1. Model equations

Momentum

$$\frac{\partial V_r}{\partial t} + V_r \frac{\partial V_r}{\partial r} + \frac{V_\theta}{r}\frac{\partial V_\theta}{\partial \theta} - \frac{V_\theta^2}{r} + V_z \frac{\partial V_r}{\partial z} = -\frac{1}{\rho}\frac{\partial P}{\partial r} + \frac{1}{\rho}\left(\frac{1}{r}\frac{\partial (r\tau_{rr})}{\partial r} + \frac{1}{r}\frac{\partial \tau_{r\theta}}{\partial \theta} - \frac{\tau_{\theta\theta}}{r} + \frac{\partial \tau_{rz}}{\partial z}\right) \quad (6)$$

$$\frac{\partial V_z}{\partial t} + V_r \frac{\partial V_z}{\partial r} + \frac{V_\theta}{r}\frac{\partial V_z}{\partial \theta} + V_z \frac{\partial V_z}{\partial z} = -\frac{1}{\rho}\frac{\partial P}{\partial z} + \frac{1}{\rho}\left(\frac{1}{r}\frac{\partial (r\tau_{rz})}{\partial r} + \frac{1}{r}\frac{\partial \tau_{z\theta}}{\partial \theta} + \frac{\partial \tau_{zz}}{\partial z}\right) \quad (7)$$

continuity

$$\frac{1}{r}\frac{\partial(rV_r)}{\partial r}+\frac{1}{r}\frac{\partial V_\theta}{\partial \theta}+\frac{\partial V_z}{\partial z}=0, \tag{8}$$

where

$$\tau_{rr}=-\mu\left[2\frac{\partial V_r}{\partial r}-\frac{2}{3}(\nabla V)\right] \tag{9}$$

$$\tau_{\theta\theta}=-\mu\left[2\left[\frac{1}{r}\frac{\partial V_\theta}{\partial \theta}+\frac{V_r}{r}\right]-\frac{2}{3}(\nabla V\ \ )\right] \tag{10}$$

$$\tau_{zz}=-\mu\left[2\frac{\partial V_z}{\partial r}-\frac{2}{3}(\nabla V)\right] \tag{11}$$

$$\tau_{r\theta}=\tau_{\theta r}=-\mu\left[\frac{1}{r}\frac{\partial V_r}{\partial \theta}+r\frac{\partial}{\partial r}\left(\frac{V_\theta}{r}\right)\right] \tag{12}$$

$$\tau_{z\theta}=\tau_{\theta z}=-\mu\left[\frac{1}{r}\frac{\partial V_z}{\partial \theta}+\frac{\partial V_\theta}{\partial z}\right] \tag{13}$$

$$\tau_{zr}=\tau_{rz}=-\mu\left[\frac{\partial V_z}{\partial r}+\frac{\partial V_r}{\partial z}\right] \tag{14}$$

$$(\nabla V)=\frac{1}{r}\frac{\partial(rV_r)}{\partial r}+\frac{1}{r}\frac{\partial V_\theta}{\partial \theta}+\frac{\partial V_z}{\partial z}, \tag{15}$$

where *V*r, V_θ and *V*z are the fluid velocities (m/s) at *r*, θ and *z* coordinates respectively, *p* is the pressure drop (Pa) and μ is the dynamic viscosity (Pa.S). Simulations are performed in two-dimension using COMSOL Multiphysics [15]. These equations are solved by using the finite element method where the equations are discretized and the regression method is used to minimize the error and converge the solution.

2.3.2. Boundary conditions

Boundary conditions for the mixing problem are

a. Time dependent inlet velocity

$$V_{in} = 2\pi A f \cos(2\pi f t)$$

b. At the outlet, pressure boundary conditions is given.
c. No Slip boundary condition is given at the walls

The working fluid is water at a room temperature (density 998.2 kg/m^3, dynamic viscosity 0.001003 kg/ms).

2.3.3. 2D cases of mixing patterns

Simulations are performed for 2D cases by solving incompressible Navier Stokes equations along with continuity equation; the geometry chosen is of single section in the column. The diameter

of the column is 50 mm. The baffle spacing is varied i.e. 50, 75, 100 mm (1, 1.5 and 2 times the diameter of column). The baffle free area considered is 22%.

3. Results and discussions

3.1. Velocity field variation with operating conditions

Figure 3 shows the streamlines, velocity vectors and surface plots for amplitude of 2 mm, frequency of 0.5 Hz and 1.5 times of diameter baffle spacing at four different time locations. Figure 3a is at the start of the oscillations, where the flow has not separated at the baffle edge. Figure 3b shows that flow has separated at baffle edge and can be manifested by vortices formation, which is sweeping the fluid/substances from the wall to bulk fluid. Figure 3c shows phase three fully reversed flow, which is similar to Figure 3a but in the opposite direction and also flow has not separated yet. Figure 3d shows phase four, where the flow has separated and eddies are sweeping the fluid from wall to bulk fluid, which increases the fluid mixing. This phenomenon will lead to an increase in transfer coefficients, which is desirable in any chemical engineering operations.

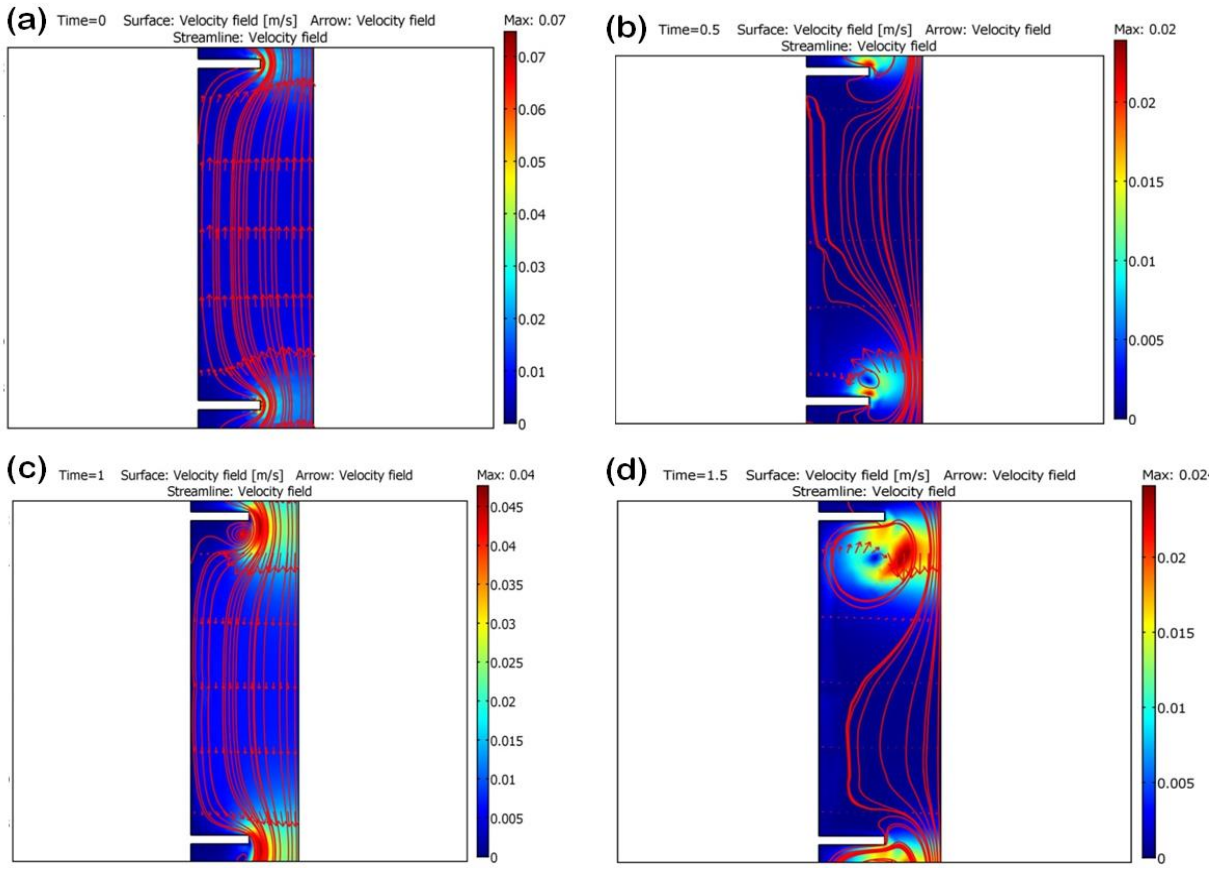

Figure 3. (a) Surface, arrow and streamlines profile for f = 0.5 Hz and A = 2 mm with time sequence of one cycle. (b) Surface, arrow and streamlines profile for f = 0.5 Hz and A = 2 mm with time sequence of one cycle. (c) Surface, arrow and streamlines profile for f = 0.5 Hz and A = 2 mm with time sequence of one cycle. (d) Surface, arrow and streamlines profile for f = 0.5 Hz and A = 2 mm with time sequence of one cycle.

Figure 4 shows the streamlines and velocity vectors and surface plots for amplitude of 2 mm, frequency of 1 Hz and 1.5 times of *d* baffle spacing at two different time locations. In Figure 4a, which is at phase two, flow has separated. In Figure 4b, which is at phase four, eddy size has remained nearly the same as in Figure 3d but magnitudes have increased.

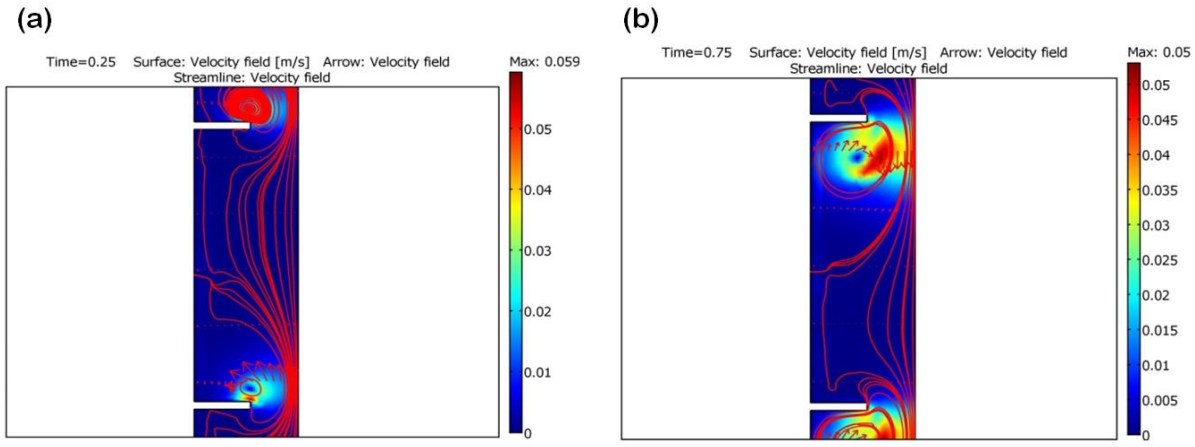

Figure 4. (a) Surface, arrow and streamlines profile for f = 1 Hz and A = 2 mm with time sequence of one cycle. (b) Surface, arrow and streamlines profile for f = 1 Hz and A = 2 mm with time sequence of one cycle.

Figure 5a, which is at phase two, shows the eddy formation as flow has separated but the remarkable feature is, small eddies have also formed in the top region which in turn enhances the mixing of the fluids, which increases the transfer coefficients. In Figure 5b, dense eddies have formed with some circulation at downstream baffle.

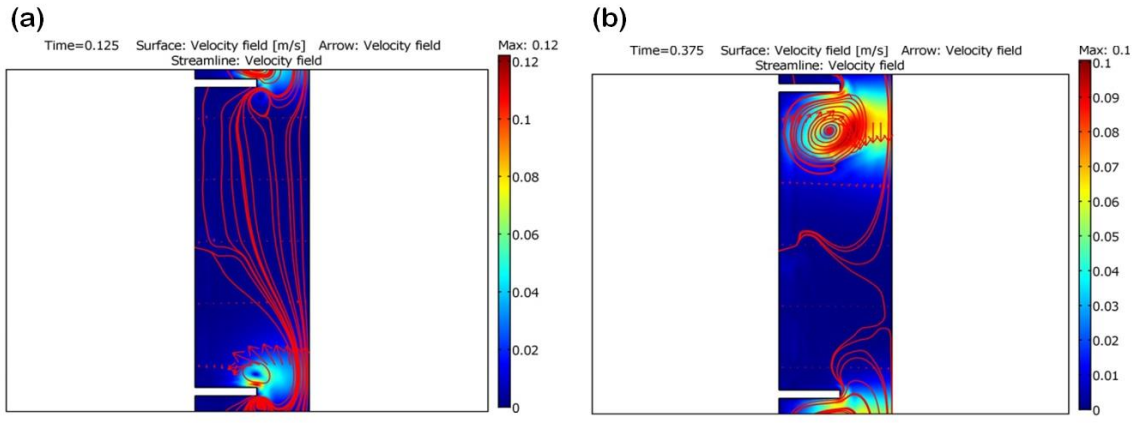

Figure 5. (a) Surface, arrow and streamlines profile for f = 2 Hz and A = 2 mm with time sequence of one cycle. (b) Surface, arrow and streamlines profile for f = 2 Hz and A = 2 mm with time sequence of one cycle.

Figure 6a is at phase three when the flow is fully reversed, and the remarkable feature is that the flow has separated which is not the case in earlier results. In Figure 6b, which is at phase two,

flow has separated and eddy size has also increased, and as a result the laminar boundary layer is destroyed or reduced leading to significant improvement in heat and mass transfer coefficients. On the negative side, this leads to an increase in pressure drop.

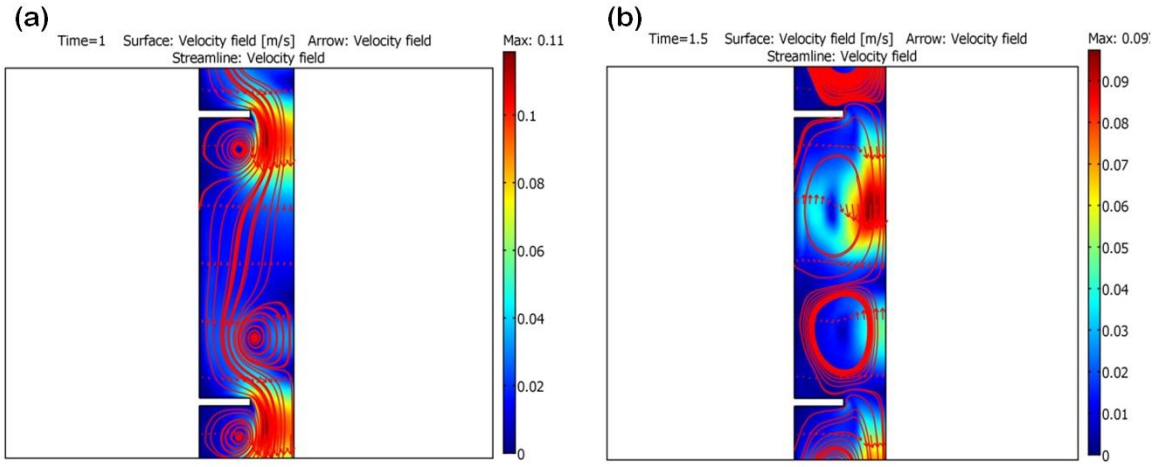

Figure 6. Surface, arrow and streamlines profile for f = 0.5 Hz and A = 5 mm with time sequence of one cycle.

In Figure 7, which is at phase four, eddy size has increased and eddies have covered the entire inter baffle region. Figure 8 is for higher frequency, where eddy size and number have increased along with magnitudes covering the whole of the inter baffle region. Figure 9 is for the frequency of 0.5 Hz and amplitude of 15 mm. Here, the size of the eddy has increased drastically and the eddy movement has also increased, covering the inter baffle region. Figure 10 is for the frequency of 2 Hz but amplitude of 15 mm, here the size of the eddy has increased drastically and the eddy has covered whole of the inter baffle region. This phenomenon increases the transfer coefficients but leads to pressure drop. Similar simulations have been performed for remaining operating parameters.

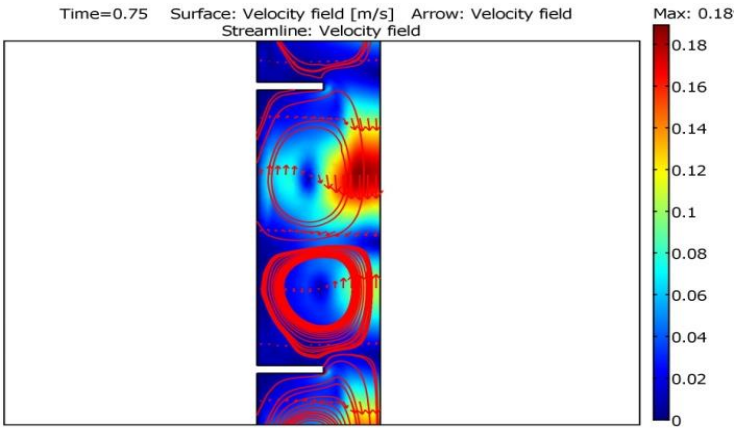

Figure 7. Surface, arrow and streamlines profile for f = 1 Hz and A = 5 mm with time sequence of one cycle.

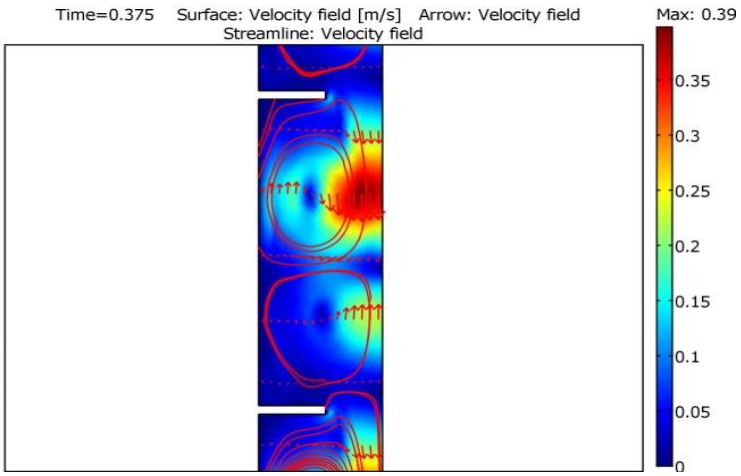

Figure 8. Surface, arrow and streamlines profile for f = 2 Hz and A = 5 mm with time sequence of one cycle.

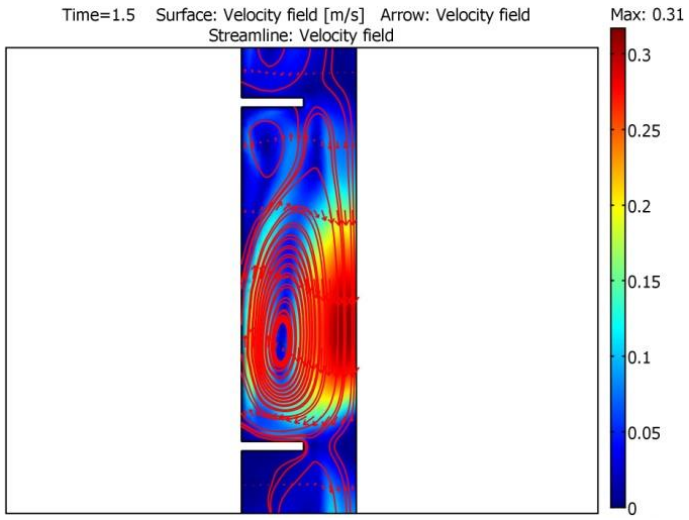

Figure 9. Surface, arrow and streamlines profile for f = 0.5 Hz and A = 15 mm with time sequence of one cycle.

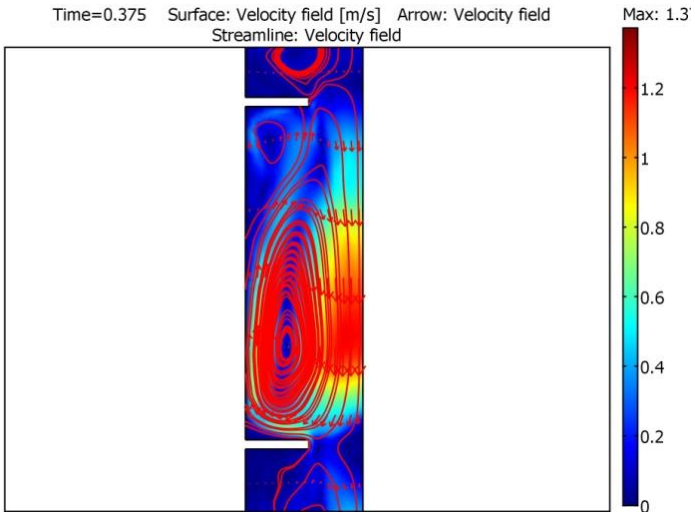

Figure 10. Surface, arrow and streamlines profile for f = 2 Hz and A = 15 mm with time sequence of one cycle.

4. Experimental studies

4.1. Residence time distribution

The residence time distribution (RTD) study gives the hydrodynamic behavior of the system [16]. RTD experiments are carried out in a metallic reactor with NaCl as tracer operated at different frequencies, amplitudes and flow rates. The experiment arrangement is shown in Figure 11. The apparatus consists of tantalum tube with internal diameter of 19.4 mm and length of 0.275 m. There are nine baffles equally spaced at a distance of 1.5 times the diameter of the tube. This spacing was optimized by [17] from the interpretation of flow visualization photographs to be the optimal baffle spacing for effective mixing over a broad range of amplitudes. The baffles are made of PTFE with 12 mm internal diameter, with 41% free cross-sectional area. Water inlet and outlet tubes are quarter inch tubes with tracer injection and sampling collection ports respectively. Flow rate was monitored with the arrangement of a flow meter at the inlet of the tube. Samples are collected at equal intervals and analyzed using automatic potentiometric titrator. To that end, 10 ml of 30 g/l NaCl tracer was injected into the tracer injection port over a period of 3–4 secs. Experiments are carried out at three different amplitudes and frequencies and two different flow rates.

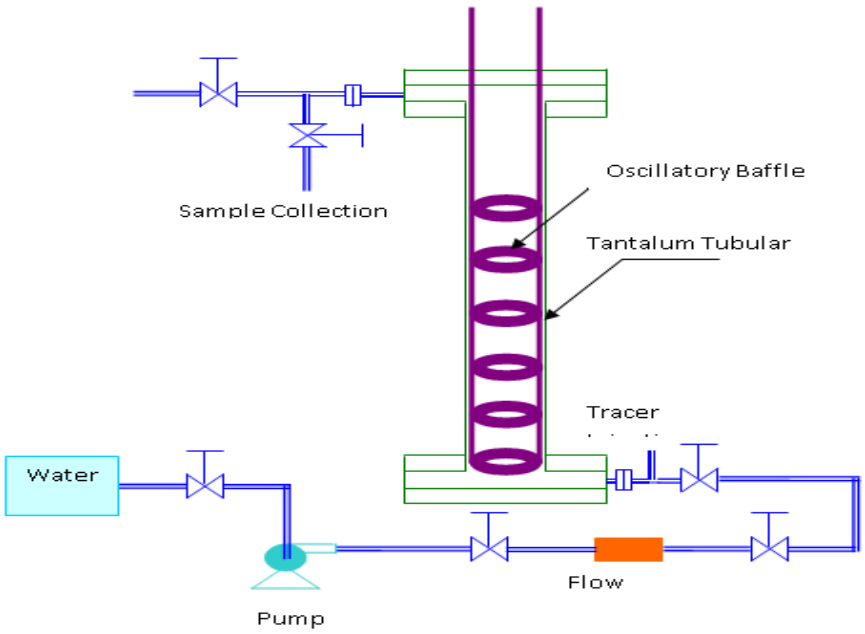

Figure 11. Experimental setup for residence time distribution.

The mixing performance of Bunsen reactor configurations can be determined by evaluating the axial dispersion coefficient, expressed as a dimensionless number, the vessel dispersion number, D/uL [14].

The mixing performance of oscillatory baffled Bunsen reactor is analyzed by the using axial dispersion model for continuous mode evaluated experimentally.

D/*uL* can be evaluated in a number of ways from an experimental curve [18]. The method which adopted here to calculate is by calculating its variance and obtaining *D/uL*.

Figure 12 shows the variation of vessel dispersion number with frequency at different amplitudes and at a flow rate of 0.12 l/m, and from the figure it can be seen that variation in vessel dispersion number is not significant with amplitude. At higher frequencies, the vessel dispersion number has increased. Figure 13 shows variation of vessel dispersion number at different amplitudes at 0.12 l/m flow rate. Here, the vessel dispersion number has remained almost constant at lower frequencies and increased at higher frequencies. In Figures 14 and 15, the vessel dispersion number has remained constant at lower frequencies but decreased at higher frequencies, and the magnitudes of vessel dispersion numbers are higher than that of Figures 12 and 13. Figure 16 shows the vessel dispersion number variation with flow rate, where it increased linearly with flow rate. For a constant column diameter, the Strouhal number is inversely proportional to amplitude. At lower flow rates, as the amplitude is decreased (means Strouhal number is increased) as shown in Figure 12, dispersion coefficient initially is increased and decreased. However, the variation of dispersion number was not significant. At higher flow rates and higher frequencies from Figure 14 of the report, dispersion coefficient is increased with the decrease in amplitude.

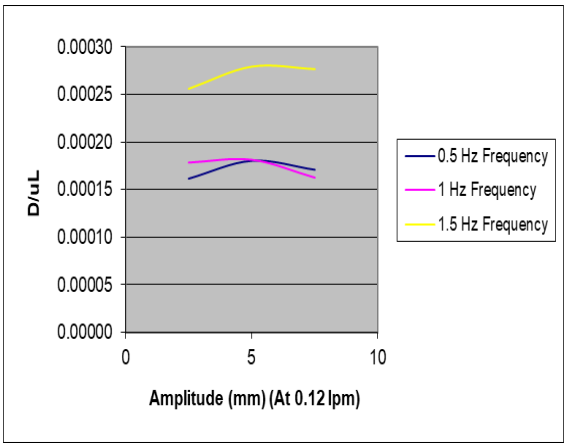

Figure 12. Vessel dispersion number variation with amplitudes at three different frequencies at a flow rate of 120 ml/m.

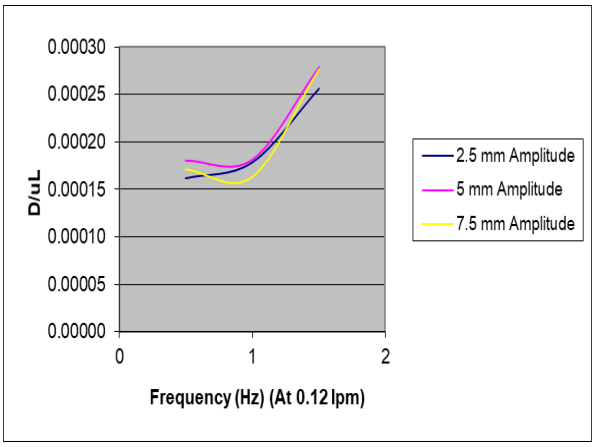

Figure 13. Vessel dispersion number variations with frequency at three different amplitudes at a flow rate of 120 ml/m.

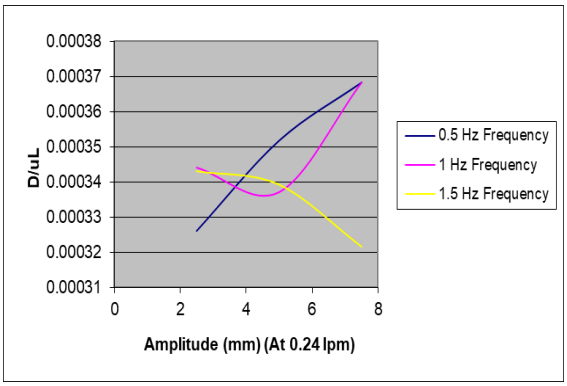

Figure 14. Vessel Dispersion number variation with amplitudes at three different frequencies at a flow rate of 240 ml/m.

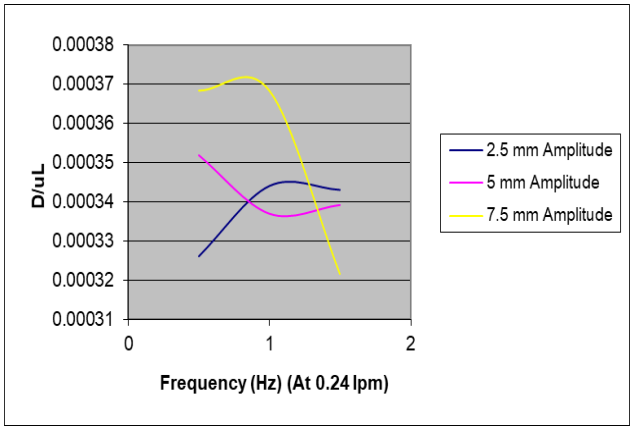

Figure 15. Vessel Dispersion number variations with frequency at three different amplitudes at a flow rate of 240 ml/m.

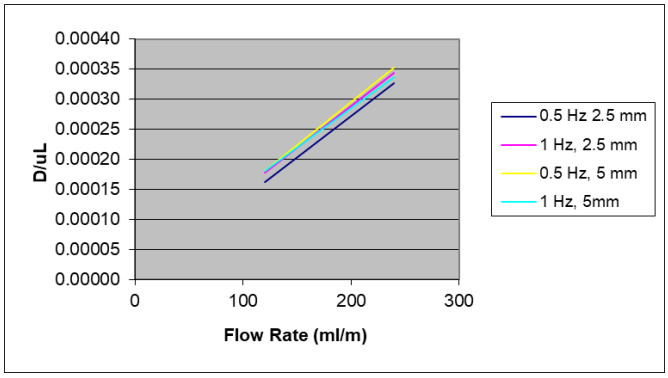

Figure 16. Vessel dispersion number variations with flow rate.

So, in view of performance of the column to achieve plug flow behavior, i.e., lower dispersion number, it is better to operate at medium frequencies and higher amplitudes (lower Strouhal number) keeping flow rate constant. If the flow rates are high, then it is better to operate at higher frequencies and higher amplitudes (lower Strouhal number) to achieve plug flow behavior. Overall, it is better to operate at higher amplitudes, i.e., lower Strouhal number, to get better performance of the column.

5. Power requirement calculations

Power per unit volume is one of the important criteria in decision making of any process equipment [19,20]. The power per unit mass is compared for oscillatory baffled column and stirred tank for a semi batch process in which sparging of gas is also considered as the Bunsen reaction involves gas sparging [19].

The equations used for calculation are shown below.

$$\frac{P}{M} = \frac{K_T n^3 d_a^5}{V} \tag{16}$$

where n is impeller rotation speed, d_a is impeller diameter, K_T is power number and V is volume of fluid in the tank.

$$(P/M)= (P/M)_B + (P/M)_O \quad (17)$$

Equation 17 is a combination of oscillatory power per unit mass and power per unit mass of rising bubbles. Oscillatory power per unit mass according to quasi steady state model is given as

$$\left(\frac{P}{M}\right)_0 = \frac{2n}{3\pi C_O^2}\frac{1-S^2}{S^2 L}A^3\omega^3 \quad (18)$$

Power per unit mass due to rising of bubble is given as

$$\left(\frac{P}{M}\right)_B = {u_{sG}}^3 \quad (19)$$

where u_{sG} is superficial gas velocity and g is acceleration due to gravity.

By considering batch volume of 500 ml, with gas flow rate of 25 cc/sec, free cross sectional area of 23 %, C_o considered as 0.7, baffle spacing of 37.5 mm and number of baffles per unit length as 150 per meter, Superficial gas velocity of 0.051 m/s, K_T is taken as 1.7, amplitude and frequency are 3mm and 4 Hz respectively and the fluid density as 1300 kg/m^3. By using the above data and calculating power per unit mass for stirred bubble column and oscillatory baffle column. The power per unit mass for stirred bubble column is 0.7226 W/Kg whereas for oscillatory baffle column it is 0.1321 W/Kg.

6. Conclusions

From the numerical simulations, it can be concluded that good eddy interactions are present at higher frequencies and amplitudes and at a baffle spacing of 1.5 times the diameter of the column, which in turn help in increasing the transfer coefficients largely.

From the residence time distribution analysis, it can be concluded that, to achieve plug flow behavior, i.e., lower dispersion number, it is better to operate at medium frequencies (1 Hz) and higher amplitudes (7.5 mm) keeping flow rate constant. If the flow rates are high, then it is better to operate at higher frequencies (1.5 Hz) and amplitudes (7.5 mm) to achieve plug flow behavior. This study is used for improving the performance of heterogeneous chemical reactions involving heat and mass transfer issues apart from chemical reaction. In the studied column, apart from better hold up and interfacial area, better radial profiles are obtained. This leads to uniformity in temperature and concentration. This subsequently improves the transport processes. This technology can be adopted for any type of application where flexibility in mode of operation of chemical reactor is desired. Thus, this equipment with this type of mixing technology can be used to facilitate process intensification and integration. Power per unit mass is less for the oscillatory baffle column compared to the stirred tank of given configuration. With better mixing performance and less power per unit volume, the oscillatory baffle column is a good alternative to other columns.

Use of AI tools declaration

The authors declare they have not used artificial intelligence (AI) tools in the creation of this article.

Acknowledgments

We thank Director, Bhabha Atomic Research Centre, Mumbai, India for encouraging above work and for the fund allocation.

Conflict of interest

The authors declare no conflict of interest in this paper.

References

1. Jain IP (2009) Hydrogen the fuel for 21st century. *Int J Hydrogen Energy* 34: 7368–7378. https://doi.org/10.1016/j.ijhydene.2009.05.093
2. Beghi GE (1986) A decade of research on thermochemical hydrogen at the Joint Research Centre, Ispra. *Int J Hydrogen Energy* 11: 761–771. https://doi.org/10.1016/0360-3199(86)90172-2
3. Lee BJ, No HC, Yoon HJ, et al. (2008) An optimal operating window for the Bunsen process in the I–S thermochemical cycle. *Int J Hydrogen Energy* 33: 2200–2210. https://doi.org/10.1016/j.ijhydene.2008.02.045
4. Ahmed VN, Rao AS, Sujeesh S, et al. (2018) Evaluation of Bunsen reaction at elevated temperature and high pressure in continuous co-current reactor in iodine-sulfur thermochemical process. *Int J Hydrogen Energy* 43: 8190–8197. https://doi.org/10.1016/j.ijhydene.2018.03.098
5. Ahmed VN, Rao AS, Sujeesh S, et al. (2017) Role of operating conditions on cross contamination of products of the Bunsen reaction in iodine-sulfur process for production of hydrogen. *Int J Hydrogen Energy* 42: 29101–29106. https://doi.org/10.1016/j.ijhydene.2017.09.133
6. Norman JH, Besenbruch GE, Brown LC, et al., Thermochemical water-splitting cycle, bench-scale investigations, and process engineering, final report for the period February 1977 through December 31, 1981. GA-A16713, 1982. Available from: https://www.osti.gov/biblio/5063416.
7. Richardson JF (2002) *Coulson & Richardson's Chemical Engineering Design*, Amsterdam: Elsevier.
8. Ni X (1995) A study of fluid dispersion in oscillatory flow through a baffled tube. *J Chem Technol Biotechnol* 64: 165–174. https://doi.org/10.1002/jctb.280640209
9. Stonestreet P, Harvey AP (2002) A mixing-based design methodology for continuous oscillatory flow reactors. *Chem Eng Res Des* 80: 31–44. https://doi.org/10.1205/026387602753393204
10. Torab-Mostaedi M, Safdari J (2009) Mass transfer coefficients in a pulsed packed extraction column. *Chem Eng Process Process Intensif* 48: 1321–1326. https://doi.org/10.1016/j.cep.2009.06.002

11. Ni X, Mackley MR, Harvey AP (2003) Mixing through oscillations and pulsations—a guide to achieving process enhancements in the chemical and process industries. *Chem Eng Res Des* 81: 373–383. https://doi.org/10.1205/02638760360596928
12. McGlone T, Briggs NEB, Clark CA, et al. (2015) Oscillatory flow reactors (OFRs) for continuous manufacturing and crystallization. *Org Process Res Dev* 19: 1186–1202. https://doi.org/10.1021/acs.oprd.5b00225
13. Ni X, Gough P (1997) On the discussion of the dimensionless groups governing oscillatory flow in a baffled tube. *Chem Eng Sci* 52: 3209–3212. https://doi.org/10.1016/S0009-2509(97)00104-8
14. Mackley MR, Ni X (1991) Mixing and dispersion in a baffled tube for steady laminar and pulsatile flow. *Chem Eng Sci* 46: 3139–3151. https://doi.org/10.1016/0009-2509(91)85017-R
15. Levenspiel O (1998) *Chemical Reaction Engineering*, 3 Eds., Hoboken: John Wiley & Sons.
16. Brunold CR, Hunns JCB, Mackley MR, et al. (1989) Experimental observations on flow patterns and energy losses for oscillatory flow in ducts containing sharp edges. *Chem Eng Sci* 44: 1227–1244. https://doi.org/10.1016/0009-2509(89)87022-8
17. COMSOL, COMSOL Multiphysics. COMSOL, n.d. Available from: https://doc.comsol.com/5.5/doc/com.comsol.help.comsol/COMSOL_ReferenceManual.pdf.
18. Zheng M, Mackley M (2008) The axial dispersion performance of an oscillatory flow meso-reactor with relevance to continuous flow operation. *Chem Eng Sci* 63: 1788–1799. https://doi.org/10.1016/j.ces.2007.12.020
19. McCabe WL, Smith JC, Harriott P (1993) *Unit Operations of Chemical Engineering*, 5 Eds., New York: McGraw-hill.
20. Baird MH, Stonestreet P (1995) Energy-dissipation in oscillatory flow within a baffled tube. *Chem Eng Res Des* 73: 503–511.

AIMS Press